

X-ray wakes as probes of galaxy cluster dynamics

Michael. R. Merrifield

*Department of Physics and Astronomy
University of Southampton,
Southampton SO17 1BJ*

23 September 2018

ABSTRACT

If a galaxy resides in a cluster, then its passage through the pervasive intracluster medium will produce a detectable signature in the X-ray emission from the cluster. Such features have now been detected in a number of systems. The simplest kinematic information that can be extracted from this signature is the galaxy’s direction of motion on the plane of the sky. This paper explores the constraints on cluster dynamics that could be derived from such information. In particular, we show that it is possible to define a projected anisotropy parameter, $B(R)$, which is directly analogous to the usual orbital anisotropy parameter. We describe an estimator for this quantity, $\hat{B}(R)$, which can be derived in a robust and straightforward manner. We present a simple dynamical model for a cluster consisting of a Michie distribution function of galaxies orbiting in a truncated singular isothermal sphere potential. Using this model, we demonstrate the ambiguity between the distribution of mass and the distribution of galaxy orbits when interpreting the traditional measures of cluster kinematics (the projected density of galaxies and their line-of-sight velocity dispersion). As an example, we show how two very different dynamical models can fit the kinematic properties of the Coma cluster. We demonstrate that the measurement of \hat{B} using a relatively small sample of wake directions ($N_{\text{wake}} \approx 50$) would provide an effective mechanism for lifting this degeneracy. Thus, by combining X-ray measurements of wake directions with number counts and line-of-sight velocities derived from optical data, it will prove possible to measure both the orbit distribution and the form of the gravitational potential in clusters of galaxies. The requisite X-ray observations lie within reach of the soon-to-be-launched AXAF satellite.

Key words: galaxies: clusters: kinematics and dynamics – galaxies: interactions – intergalactic medium – X-rays: galaxies – galaxies: clusters: individual: Abell 1656

1 INTRODUCTION

As the seminal work on the Coma cluster by Kent & Gunn (1982) first demonstrated, it is possible to study the dynamics of a cluster of galaxies by combining photometric observations of the galaxies’ positions on the plane of the sky with spectroscopic measurements that reveal the line-of-sight velocities of cluster members. If it is assumed that the cluster is spherically symmetric, these observed properties can usefully be quantified by the projected number density of galaxies as a function of projected radius, $N(R)$, and the RMS dispersion in the galaxies’ line-of-sight velocities as a function of projected radius, $\sigma_{\text{los}}(R)$. Dynamical models with different distributions of galaxy orbits can then be tested against the observations by comparing $N(R)$ and $\sigma_{\text{los}}(R)$ to the forms for these functions that the models predict.

In principle, such a study allows us to investigate the manner in which a cluster has formed and evolved. Galaxies have relatively long dynamical “memories,” and so their current orbits must to some degree reflect the processes by which the cluster formed. For example, if the galaxies are found to follow preferentially radial orbits, then their motions presumably reflect the radial infall from which the cluster originally formed. Further, the kinematics of the galaxies are dictated by the gravitational potential of the cluster as a function of radius, $\Phi(r)$, and so dynamical modelling allows us to probe the distribution of mass in the cluster. Since the mass of a galaxy cluster is dominated by dark matter, no study of the evolution of such a system is complete without addressing the distribution of this massive component as inferred from the gravitational potential.

Unfortunately, there is a fundamental ambiguity in such studies. As Binney & Mamon (1982) demonstrated, for any

arXiv:astro-ph/9710238v1 22 Oct 1997

given $\Phi(r)$ it is possible to reproduce a wide range of functions $N(R)$ and $\sigma_{\text{los}}(R)$ simply by varying the balance between radial and tangential motions in the orbits that the galaxies follow. They parameterized this balance by the anisotropy parameter,

$$\beta(r) = 1 - \frac{\sigma_t^2}{\sigma_r^2}, \quad (1)$$

where σ_t and σ_r are the RMS velocities in the tangential and radial directions for galaxies at radius r in the cluster.* Thus, it is not possible to use just $N(R)$ and $\sigma_{\text{los}}(R)$ to solve for both $\Phi(r)$ and $\beta(r)$.

One approach to lifting this degeneracy is to find some independent technique for measuring $\Phi(r)$, and then use $N(R)$ and $\sigma_{\text{los}}(R)$ to solve for the orbital anisotropy, $\beta(r)$. For example, the form of the gravitational potential can be inferred from the properties of the X-ray emitting intracluster medium (ICM). By measuring the temperature of this hot gas and its spatial distribution using an X-ray telescope, it is possible to solve uniquely for the form of the gravitational potential that contains the gas – see, for example, Eyles et al. (1991). Alternatively, one can use the distortion of optical images of background galaxies due to the gravitational lensing effects of the cluster mass to measure $\Phi(r)$ directly (Tyson, Wenk & Valdes 1990).

In practice, neither of these techniques is entirely satisfactory. The measurement of $\Phi(r)$ using X-ray data requires one to measure the temperature profile of the ICM as well as its density profile, and the poor spatial and spectral resolution and limited sensitivity of existing X-ray observations make this a difficult task. The inversion from gravitational lens distortions to $\Phi(r)$ can only be made if the distorted shapes of many background galaxies are measured, and is to some extent dependent on the assumed redshift distribution of the background galaxies. Further, neither of these techniques is well-suited to measuring $\Phi(R)$ in poorer clusters, where the X-ray emission will be weak, and the amount of gravitational-lens distortion will be small.

Perhaps this problem can be more profitably attacked from the other direction: if we can find some additional constraint on the distribution of orbits in a cluster, then we can use this information to lift the ambiguity and solve for both the galaxy kinematics and the cluster potential. One attempt to adopt this approach was made by Merritt (1987). In a further study of the Coma cluster’s kinematics, he showed that the distribution of member galaxies’ line-of-sight velocities will have a shape that may depart dramatically from a Gaussian depending on the distribution of galaxy orbits. Specifically, if the orbits are preferentially radial then the the velocity distribution will have longer tails than a Gaussian, while if the orbits are more circular it will have a “boxier” appearance. This information in the shape of the line-of-sight velocity distribution has been successfully exploited in dynamical studies of the stars in individual galaxies (e.g. van der Marel & Franx 1993, Kuijken & Merrifield 1993), but it has proved less useful in the case of clusters. The main difficulty in using the shape of a cluster’s

velocity distribution is that clusters are not entirely relaxed systems. A relatively small amount of substructure in the distribution of galaxy velocities within a cluster, perhaps due to an infalling group of galaxies that has yet to disrupt completely, can totally dominate the departures from a Gaussian in the line-of-sight velocity distribution (Zabludoff, Franx & Geller 1993).

In this paper, we explore an alternative candidate for the requisite kinematic constraint: the X-ray signature of the interactions between cluster galaxies and the surrounding ICM. As a galaxy moves through the ICM, the combination of gravitational focusing of the ICM and ram pressure stripping of the galaxy’s own interstellar medium (ISM) will produce an enhancement in the density of gas behind the galaxy – see Balsara, Livio & O’Dea (1994) for a review of these processes and the results of some simulations. Thus, we expect a galaxy’s direction of motion on the plane of the sky to be marked out in X-ray observations by a “wake” of excess emission trailing behind it. This phenomenon has now been observed in several systems. Sakelliou, Merrifield & McHardy (1997) found a wake of X-ray emission emanating from the radio galaxy 4C34.16. In this case, the bent morphology of the radio jets provides a further measure of the galaxy’s direction of travel, and the wake is found to lie downstream from the moving galaxy. A further example is provided by the dumb-bell galaxy NGC 4782/3 (Colina & Borne 1995). In this interacting pair of elliptical galaxies, the X-ray emission from the individual components is offset from the optical light produced by the galaxies in the sense that one would expect if it were trailing behind the orbiting galaxies. The X-ray emission also reveals more extended wake features lagging behind the orbiting components. Finally, Jones et al. (1997) have found that the X-ray emission from the elliptical galaxy NGC 1404 is strongly distorted, forming a wake pointing away from the centre of the Fornax cluster in which it resides. They suggest that this X-ray morphology arises from the ram pressure stripping of the galaxy’s ISM, and hence conclude that NGC 1404 is on a plunging radial orbit.

With the advent of more sensitive X-ray telescopes such as XMM and high resolution imaging instruments such as AXAF, the detection of these wake phenomena can only become more commonplace, and we might reasonably expect to be able to use wakes as a probe of the kinematics of many galaxies within a single cluster. For example, Balsara et al. (1994) have calculated that at the distance of the Coma cluster one might expect to see many wake structures with extents of ~ 2 arcseconds – a scale readily resolvable with AXAF.

In principle, a great deal of information can be gleaned from the pattern of shocks and other structure present in X-ray wakes. However, in addition to the velocity of the galaxy, this structure depends in a complex manner on the properties of the ICM, how much of the galaxy’s ISM has already been stripped away, how rapidly the ISM is being replenished by stellar mass loss within the galaxy, etc. We therefore content ourselves with using the X-ray morphology to measure the direction in which each galaxy is moving on the plane of the sky. In the remainder of this paper, we investigate whether such information is sufficient to lift the degeneracy between orbital anisotropy and gravitational potential. In Section 2, we present a practical measure of

* Note that there are two equal tangential components in a spherical system (in the θ and ϕ directions of a spherical polar coordinate system), and so σ_t^2 is sometimes defined to be a factor of two larger.

the orbital structure that can be determined directly from the observed wake directions in a cluster. Section 3 presents a simple dynamical model, which illustrates how the proposed measure of orbital structure can discriminate between otherwise-indistinguishable models.

2 ESTIMATING THE PROJECTED ANISOTROPY

The direction in which the wakes in a cluster trail on the sky clearly tells us something about the distribution of orbits. Suppose, for example, that the wakes imply that all the galaxies in the cluster are moving either directly toward or away from the cluster centre in the plane of the sky. The only spherically-symmetric system that could produce such an arrangement of projected motions is one in which the galaxies are all on intrinsically radial orbits. Thus, in this case at least, the distribution of wake directions is sufficient to define the distribution of orbits uniquely. Note, however, that the relation between the wake directions and orbital anisotropy is not completely trivial: if all the galaxies follow circular orbits, the wakes will *not* all be tangentially-oriented on the plane of the sky, and some will still appear pointed at the cluster centre.

In order to explore the relationship between wake directions and orbital distribution more fully, it is useful to define a “projected anisotropy.” By analogy with equation (1), an obvious definition for this quantity is

$$B(R) = 1 - \frac{\sigma_T^2}{\sigma_R^2}, \quad (2)$$

where $\sigma_T(R)$ and $\sigma_R(R)$ are the RMS velocities of galaxies on the plane of the sky in the projected tangential and radial directions, respectively.

The projected anisotropy cannot be measured directly, but we can estimate it from the observed distribution of projected orbit directions. If we define Θ to be the angle between the direction of a galaxy’s motion on the plane of the sky (as inferred from its wake) and the projected radius vector of the galaxy, then the quantity that we can observe directly is the distribution of projected orbit directions as a function of projected radius, $P(\Theta, R)$. This quantity can be related directly to $B(R)$. For example, let us assume that at some projected radius in the cluster, the plane-of-sky velocity distribution (POSVD) can be approximated by a function of the general form

$$F(v_R, v_T) = F(v_R^2/a^2 + v_T^2/b^2), \quad (3)$$

where a and b are constants. By transforming from the coordinates $\{v_R, v_T\}$ to polar coordinates on the plane of the sky, $\{v_{\text{pos}}, \Theta\}$, it is straightforward to show that the distribution of observed values of Θ will be

$$P(\Theta) = \frac{\sqrt{1-B}}{2\pi(1-B\cos^2\Theta)}. \quad (4)$$

Thus, we can estimate B by fitting the functional form of equation (4) to the observed distribution for $P(\Theta)$ at any given projected radius.

One robust method for implementing this fitting procedure is to measure the fraction of galaxies for which $\pi/4 < \Theta < 3\pi/4$ or $5\pi/4 < \Theta < 7\pi/4$. This quantity,

f_T , measures the fraction of galaxies whose orbits are closer to tangential than radial on the plane of the sky. By integrating equation (4), it is straightforward to show that the value of B that gives rise to a particular value of f_T is

$$\hat{B} = 1 - \tan^2\left(\frac{\pi}{2}f_T\right). \quad (5)$$

Thus, by measuring f_T , we can use equation (5) to estimate the projected anisotropy. This estimator for B has a number of desirable properties: it can be readily calculated from observed wake directions; it is robust in the sense that a small fraction of badly-determined directions will not affect it unduly; and it has error properties which can be determined straightforwardly from the binomial distribution of f_T .

Strictly speaking, \hat{B} is only an unbiased estimator for B if the POSVD takes the elliptical form of equation (3). However, a rather wide range of plausible models can be approximated in this way (see below). Even in cases where this approximation is not valid, \hat{B} still provides a quantity that can be readily determined not only for observational data, but also for dynamical models containing different orbit distributions. Thus, by comparing the observed profile $\hat{B}(R)$ to that predicted by a dynamical model, it is possible to test the model against observation.

3 CASE STUDY: THE MICHIE/TRUNCATED SINGULAR ISOTHERMAL SPHERE MODEL

To see how useful $\hat{B}(R)$ might prove as a diagnostic of orbital structure, we now consider a simple family of dynamical models. Such models are defined by the distribution function for the cluster, f , which specifies the density of galaxies as a function of both velocity and position (i.e. the phase density) – see Binney & Tremaine (1987) for a thorough discussion of distribution functions. By Jeans theorem, for a spherical system in equilibrium, the distribution function depends only on the energy, E , and angular momentum, J , of the point in phase space under consideration. A relatively simple distribution function that might approximate the properties of a real cluster of galaxies is the Michie model,

$$f(E, J) = \begin{cases} \text{const.}[e^{-E/\sigma_0^2} - 1]e^{-J^2/(2\sigma_0^2r_a^2)} & E < 0 \\ 0 & \text{otherwise,} \end{cases} \quad (6)$$

where σ_0 and r_a are constants (Michie 1963, Binney & Tremaine 1987). This function produces a model where the distribution of orbits is isotropic at small radii, but becomes radial at large radii. Thus, it mimics what we might expect in a cluster of galaxies: relaxation effects will have randomized the orbits at small radii in the cluster, but galaxies that travel to large radii will not have relaxed, and so their orbits will still reflect the radial infall by which the cluster formed. The quantity r_a defines the characteristic radius at which the transition from isotropic to radial orbits occurs.

The other dynamical quantity that we must specify for this model cluster is the gravitational potential, $\Phi(r)$, by which the galaxies are confined. Since clusters of galaxies are dominated by dark matter, and since we are interested in varying the orbital anisotropy and gravitational potential independently, we do not make the customary assumption that mass follows light. Instead, we impose an external gravitational potential, and vary its parameters to assess the im-

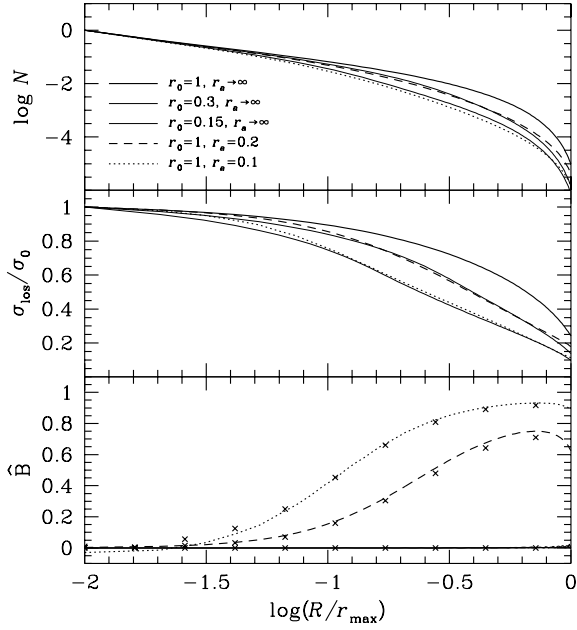


Figure 1. The observable kinematics for the dynamical models discussed in the text (with parameters r_0 and r_a as annotated). Plotted as functions of projected radii, the upper panel shows projected density, and the middle panel shows the line-of-sight velocity dispersion. The lower panel shows the projected anisotropy: the lines show the estimator calculated using equation (5), while the crosses mark the corresponding true projected anisotropy [equation (2)]. The central projected densities and line-of-sight velocity dispersions have been scaled to a common value.

pect of changing the distribution of mass in the cluster. The simplest potential that enables us to carry out such an investigation is the truncated singular isothermal sphere (TSIS), which is produced by a mass density distribution

$$\rho(r) = \begin{cases} \sigma_0^2 / (2\pi G r^2) & r < r_0 \\ 0 & \text{otherwise,} \end{cases} \quad (7)$$

where the constant σ_0 sets a characteristic velocity scale for this potential.[†] The TSIS density distribution produces a gravitational potential

$$\Phi(r) = \begin{cases} 2\sigma_0^2 \left[\ln\left(\frac{r}{r_0}\right) + \frac{r_0}{r_{\max}} - 1 \right] & r < r_0 \\ -2\sigma_0^2 r_0 \left(\frac{1}{r} - \frac{1}{r_{\max}} \right) & \text{otherwise.} \end{cases} \quad (8)$$

Here, we have set the arbitrary constant offset in the potential such that $\Phi(r > r_{\max}) > 0$. Thus, from equation (6), all the members of the cluster in this model are confined to the region $r < r_{\max}$.

Given f and Φ , we can calculate the density and velocity distribution of galaxies at any point in the cluster. It is thus straightforward to calculate observable quantities – such as $N(R)$, $\sigma_{\text{los}}(R)$, and the projected anisotropy estimator $\hat{B}(R)$ – by integrating the properties of the cluster along lines of sight through the system at different projected radii R . Figure 1 shows the results for a set of such calculations for

[†] There is no fundamental reason why this characteristic velocity should be the same as the one in equation (6), but we adopt this value as the simplest choice.

the Michie distribution function in the TSIS potential. The spatial scale has been set by defining $r_{\max} = 1$, and various combinations of the mass cut-off radius, r_0 , and the orbital anisotropy radius, r_a , have been adopted.

For the case $\{r_0 = 1, r_a \rightarrow \infty\}$, the mass cut-off has no impact (since it lies outside the cluster), and so the potential is that of a singular isothermal sphere. At small radii, the Michie distribution function is indistinguishable from an isothermal distribution function, and so the cluster itself mimics a singular isothermal sphere, with $N \propto R^{-1}$ and σ_{los} approximately constant. At larger radii, the more energetic galaxies, which would have been included in an isothermal distribution, are excluded from the Michie model, and so N drops faster than R^{-1} , and σ_{los} starts to fall. Both these quantities reach zero at $R = r_{\max}$, where the cluster ends.

As r_0 is decreased, the truncation of the mass distribution affects both N and σ_{los} . The models with $r_0 = 0.3$ and $r_0 = 0.15$ have insufficient mass to contain the highest-velocity cluster members, and so the density profile and the velocity dispersion both drop more rapidly with radius. Thus, both the dispersion profile and density profile decline rapidly when the edge of the mass distribution is reached.

However, as discussed in the introduction, the observed kinematics are affected by orbital anisotropy as well as the shape of the potential. As Fig. 1 illustrates, when r_a is reduced to a finite value, the absence of galaxies on tangential orbits at large radii means that the projected density drops more rapidly than for the isotropic case. Further, since galaxies on radial orbits travel mostly transverse to the line-of-sight when seen at large projected radii, the observed line-of-sight velocity dispersion is also depressed.

In fact, as Fig. 1 shows, it is possible to produce very similar profiles for $N(R)$ and $\sigma_{\text{los}}(R)$ using very different combinations of r_0 and r_a . In the case of the $\{r_0 = 1.0, r_a = 0.1\}$ and the $\{r_0 = 0.15, r_a \rightarrow \infty\}$ models, for example, the values of N differ by less than $\sim 10\%$ inside $R = 0.8r_{\max}$. Within this radius, the values of σ_{los} returned by the two models differ by less than 5%. Models with less extreme choices of these parameters, which include both a cut-off in the density profile and some degree of orbital anisotropy, differ even less.

The futility of trying to distinguish between such models is illustrated in Fig. 2. This figure shows the kinematic properties of the Coma cluster as derived by Kent & Gunn (1982) using line-of-sight velocities of more than 200 galaxies, with two of the models from Fig. 1 superimposed. It should be stressed that these models have not been formally fitted to the data, but rather they are simply the arbitrarily-chosen models calculated above, with their number-, velocity-, and length-scales chosen to match the observations. Indeed, it would appear that the models fail to reproduce the observed flattening of the density profile at small radii. However, Beers & Tonry (1986) have shown that such a flat core is an artifact that arises from errors in the choice of cluster centre. With the centres measured correctly, they discovered that the projected density profiles of most clusters contain no core at small radii, but continue to rise in a power-law cusp, $N \propto R^{-1}$, just as the models do. What is clear from Fig. 2 is that there is no way that the very different dynamical models can be discriminated between on the basis of these data. With very much larger data sets, the error bars could be beaten down to a point where the

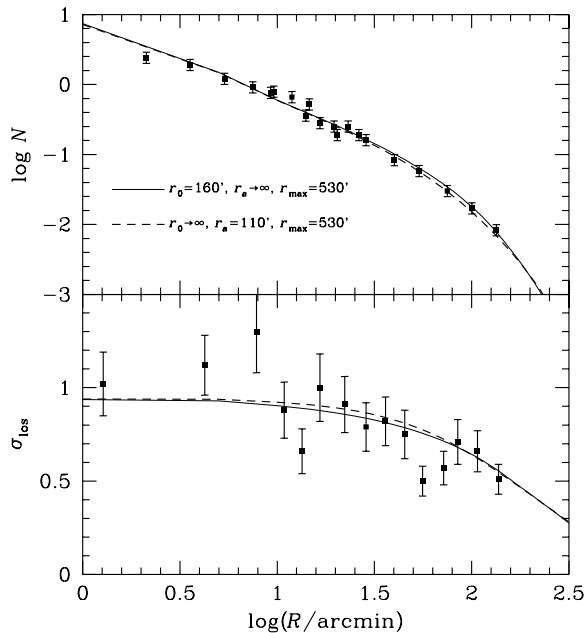


Figure 2. The projected density and line-of-sight velocity dispersion as a function of projected radius for Coma cluster galaxies (Kent & Gunn 1982) as compared to two of the models discussed in the text.

differences might become significant. However, it is already apparent from the lower panel of Fig. 2 that there are likely to be systematic errors in the observed properties: modest amounts of substructure in the cluster will mean that the simple spherically-symmetric model is at some level invalid, and contamination by unrelated galaxies along the line of sight may bias the derived properties. The presence of these fundamental systematic uncertainties means that the collection of the vast data set necessary to beat down the random errors would be a nugatory exercise.

Figure 1 shows how the measurements of wake directions, and hence $\hat{B}(R)$, might be used to lift this effective degeneracy between the different dynamical models. For the models in which $r_a \rightarrow \infty$, the distribution of orbits is isotropic at every point in the cluster. Thus, in these cases there are as many galaxies moving on radial orbits as tangential ones on the plane of the sky, the distribution of wake directions is isotropic, and hence $\hat{B} \equiv 0$. However, for the models with finite values of r_a , the radial orientation of the orbits is directly reflected by the positive values of the projected anisotropy parameter. Although the POSVD in this model is not of the form specified by equation (3), it is clear that $\hat{B}(R)$ is nonetheless a good approximation to $B(R)$ for this moderately-realistic distribution function; the two quantities never differ by more than $\sim 10\%$. Thus, the observable $\hat{B}(R)$ does provide a useful measure of the underlying projected anisotropy.

The finite values of \hat{B} predicted by the anisotropic models would be readily detectable with relatively small samples of wake directions. If, for example, we assume that the cluster is isotropic, then $f_T = 0.5$, and we can apply binomial statistics to show that a sample of N_{wake} measured wake directions will produce an estimate for this quantity of $\hat{f}_T = 0.5 \pm 0.5/\sqrt{N_{\text{wake}}}$. The value of $\hat{B} \approx 0.7$ in

the anisotropic models shown in Figure 1 corresponds to $f_T \approx 0.3$. Thus, if the cluster were in reality better modeled by one of these anisotropic systems, then a sample of only $N_{\text{wake}} \approx 50$ wake directions drawn from projected radii where $\hat{B} \approx 0.7$ would be sufficient to rule out the isotropic $f_T = 0.5$ model at the 3σ level.

4 DISCUSSION

The passage of a galaxy through its host cluster must have some impact on the distribution of the gas in its vicinity, and we are now finding the first signs of these effects in X-ray observations. The purpose of this paper has been to address the question of whether the simplest kinematic information that can be extracted from observations of this phenomenon – the distribution of directions of galaxy motion on the plane of the sky – can be useful in dynamical studies of clusters. By means of the simple Michie/TSIS model, we have shown that such observations can readily discriminate between models that have different underlying orbit distributions and gravitational potentials, but that are indistinguishable using traditional kinematic analyses.

In practice, the proposed measure of orbital anisotropy on the plane of the sky, $\hat{B}(R)$, may not make optimal use of the observations, since it requires that we bin the data radially. It also discards any information that might be gleaned from coupling between directions on the plane of the sky and line-of-sight velocities: it is, for example, possible that galaxies with the largest velocities might lie preferentially on radial orbits, and so there might be a positive correlation between line-of-sight velocity and how close a galaxy’s orbit is to radial on the plane of the sky. It would be straightforward to exploit this information by doing a full maximum likelihood fit to the observed wake directions and line-of-sight velocities of a sample of galaxies in a cluster. The advantage of the approach adopted here is that \hat{B} can be calculated in a manner that is robust against the effects of a few bad data points, while such erroneous data could seriously compromise a maximum likelihood analysis. Further, the close tie between $\hat{B}(R)$ and the intrinsic anisotropy parameter, $\beta(r)$, means that this simple-to-measure quantity can readily be interpreted in terms of the orbital properties of the cluster.

It is interesting to note that the signature of anisotropy in a cluster is likely to be found at large radii (see Fig. 1). This radial dependence is fortunate, since it will be easiest to detect a wake near the outskirts of the cluster, where we are not viewing the interactions between the galaxy and the ICM through a large column of unrelated X-ray emitting gas. Similarly, this technique is particularly appropriate to poor systems, where the column of ICM along the line of sight is relatively small. Further, in poorer systems the energy density stored in the ICM is lower, and so the disturbance caused by the passage of a galaxy will be larger and hence more readily detectable. It is also noteworthy that contamination by non-cluster galaxies along the line of sight is one of the major problems that dogs studies of low density regions such as poor clusters and the outskirts of rich clusters. Since such unrelated galaxies will not interact with the ICM, it will be possible to screen them out from the proposed studies based on their lack of wakes. The applicability of the technique to large radii in rich clusters and to poor

clusters is particularly exciting, since, as was discussed in the introduction, it is in exactly these areas that the existing methods for mapping the gravitational potential break down.

One possible difficulty in using wake directions to study cluster dynamics is that the detectability of a wake may vary systematically with the dynamics of the galaxy producing it. For example, galaxies traveling rapidly through the cluster will produce longer and more dramatic wake phenomena, which will be easier to observe. Similarly, galaxies that have only recently joined the cluster are more likely to contain a significant ISM, which will be readily detectable as a wake of stripped material. This possible bias can be minimized by obtaining as deep an X-ray image as possible, so that even the fainter wakes are detected. Fortunately, an imaging X-ray telescope will record many wakes simultaneously, and so the mapping process can be carried out efficiently in few exposures. Hopefully, with its high spatial resolution and sensitivity, AXAF will open this new window on the dynamics of clusters of galaxies.

ACKNOWLEDGEMENTS

The author gratefully acknowledges the support of a PPARC Advanced Fellowship (B/94/AF/1840).

REFERENCES

- Balsara, D., Livio, M. & O'Dea, C.P., 1994, *ApJ*, 487, 83
 Beers, T.C. & Tonry, J.L., 1986, *ApJ*, 300, 557
 Binney, J. & Mamon, G.A., 1982, *MNRAS*, 200, 361
 Binney, J. & Tremaine, S., 1987, *Galactic Dynamics*. Princeton University Press, New Jersey
 Colina, L. & Borne, K.D., 1995, *ApJ*, 454, L101
 Eyles, C.J., et al., 1991, *ApJ*, 376, 23
 Jones, C., et al., 1997, *ApJ*, 482, 143
 Kent, S.M. & Gunn, J.E., 1982, *AJ*, 87, 945
 Kuijken, K. & Merrifield, M.R., 1993, *MNRAS*, 264, 712
 Merritt, D., 1987, *ApJ*, 313, 121
 Michie, R.W., 1963, *MNRAS*, 125, 127
 Sakelliou I., Merrifield M. R., McHardy I. M., 1996, *MNRAS*, 283, 673
 Tyson, J.A., Wenk, R.A. & Valdez, F., 1990, *ApJ*, 349, L1
 van der Marel, R.P. & Franx, M., 1993, *ApJ*, 497, 525
 Zabludoff, A.I., Franx, M. & Geller, M.J., 1993, *ApJ*, 419, 47